Cross sections for electron-impact single ionization of Kr^{8+} and Xe^{8+}

M. E. Bannister*
Physics Division, Oak Ridge National Laboratory, Oak Ridge, Tennessee 37831-6372

D. W. Mueller†
Department of Physics and Astronomy, Louisiana State University, Baton Rouge, Louisiana 70803

L. J. Wang,‡ M. S. Pindzola,§ D. C. Griffin,** and D. C. Gregory
Physics Division, Oak Ridge National Laboratory, Oak Ridge, Tennessee 37831-6372
(Received 16 February 1988)

Absolute cross sections for electron-impact single ionization of Kr^{8+} and Xe^{8+} ions were measured for energies below the ionization thresholds to 1500 eV using the crossed-beams method. A significant fraction of the Kr^{8+} and Xe^{8+} ion beams were in metastable configurations. Configuration-average distorted-wave calculations for ions in the ground and first-excited configurations are compared to the experimental data. For both ions in this study, the excitation-autoionization contribution to the total ionization cross section is found to be much larger for ions in the first-excited configuration, which includes metastable levels, than for the ground-state ions. Maxwellian rate coefficients were calculated for Kr^{8+} and are compared to published results.

I. INTRODUCTION

Electron-impact ionization cross sections for multiply charged ions are essential for the modeling of laboratory and astrophysical plasmas, especially equal-temperature plasmas in which electron-ion collisions tend to dominate over ion-ion collisions. The cross sections are needed to calculate power balance, the effective charge Z_{eff}, impurity composition and transport, and to interpret spectroscopic diagnostics. The modeling of x-ray lasers also requires such cross sections.

One of the most popular sources of cross sections for multiply charged ions is the semiempirical one-parameter formula of Lotz,[1] which only accounts for direct ionization of the target ion. In many cases, however, the cross section due to indirect processes such as excitation autoionization (EA) can be comparable to or even exceed that due to direct processes,[2] especially at energies just above the threshold for direct ionization.

The present experiment extends the charge states of krypton and xenon for which electron-impact single-ionization cross sections have been reported. Several groups have reported single-ionization cross sections for charge states as high as $3+$ for krypton,[3-7] and others as high as $6+$ for xenon.[3,5,8-10] For both isonuclear sequences, excitation autoionization was found to be an important process. Interest in the single-ionization cross section of Kr^{8+} was stimulated by the recent use of other Ni-like ions ($3d^{10}$ outer electron configuration) to produce x-ray lasing;[11,12] the ionization cross section for Xe^{8+} was measured in order to investigate a prediction[13] of irregularities in the scaling of direct ionization in the palladium isoelectronic sequence ($4d^{10}$ outer-electron configuration). Our experimental results are compared to distorted-wave (DW) calculations for ions in the ground and first-excited configurations in order to evaluate the importance of excitation-autoionization (EA) for Kr^{8+} and Xe^{8+}.

The only published experimental work involving ionization of either of these ions to which the present results may be compared are the plasma ionization rate measurements for Kr^{8+} by Jones and Källne.[14] Their results were 2.5 times larger than that predicted by the semiempirical theory of Kunze.[15] It was suggested by Jones and Källne that the discrepancy might be due to significant excitation-autoionization contributions to the total ionization cross section.

II. EXPERIMENTAL TECHNIQUE

The measurements were performed with crossed beams of ions from the Oak Ridge National Laboratory electron cyclotron resonance (ECR) plasma ion source[16] and magnetically confined electrons from a gun similar to that of Taylor *et al.*[17] The ions of interest were extracted from a nitrogen-krypton or nitrogen-xenon plasma, accelerated through a 10-kV potential, and focused into a beam. The beam was then magnetically mass-to-charge-ratio analyzed and transported to the collision chamber shown in Fig. 1. In the chamber the incident ion beam was focused and electrostatically energy analyzed before entering the collision volume. The $8+$ and $9+$ ions leaving the collision volume were magnetically separated; the primary $8+$ ions were collected in a Faraday cup, while the $9+$ ions were electrostatically deflected by an additional 90° analyzer and detected by a channel-electron multiplier. The electron beam was chopped to allow separation of signal and noise. Beam profiles and overlaps, detector efficiency, and total electron and ion beam currents were measured in order to determine the absolute cross sections.

The uncertainties listed and plotted here reflect one-

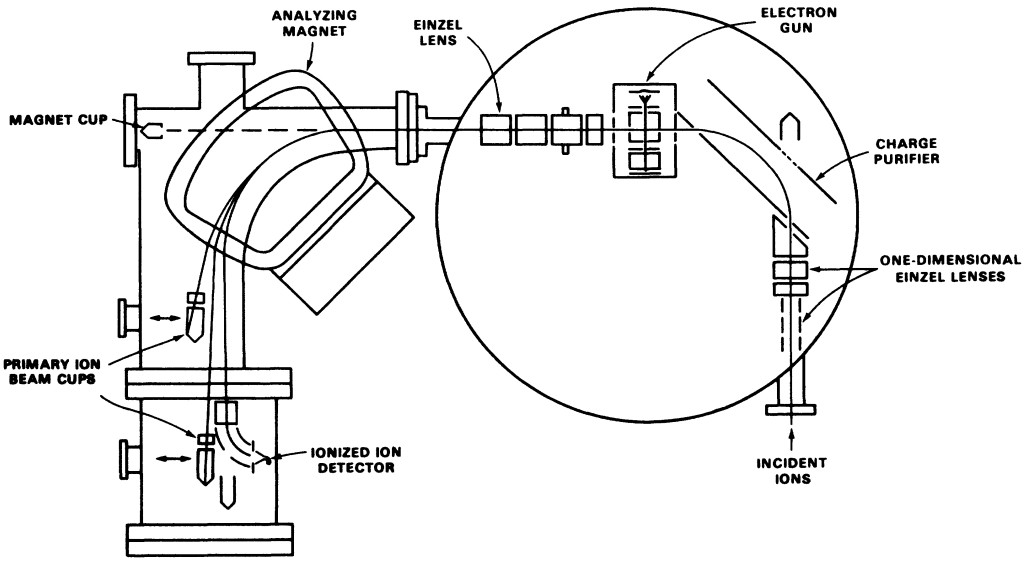

FIG. 1. Schematic of the Oak Ridge National Laboratory (ORNL) crossed-beams collision chamber and post-collision magnetic charge analyzer.

standard-deviation (or equivalent) relative uncertainties only, combining statistics and form factor instabilities. The shape of the cross section curve is determined within these uncertainties. The total absolute experimental uncertainty at 90% confidence level for data near the peak cross section is ±8%. The absolute uncertainty combines the relative uncertainty with additional potential sources of error (e.g., ion and electron velocity and current measurements, detector efficiency, and transmission of ions to the detector) which would affect each measurement the same. A detailed discussion of the absolute uncertainty and additional experimental details can be found elsewhere.[18]

III. CALCULATIONAL PROCEDURE

The cross sections for electron-impact direct ionization of ions in the ground and first-excited configurations of Kr^{8+} and Xe^{8+} were calculated using the configuration-average distorted-wave approximation method.[19,20] The calculations for the first-excited configurations were included in order to evaluate the importance of metastable ions in these experiments since these configurations contain levels which are metastable on the time scale of the experiment. The configuration-average subshell ionization potentials were obtained with the relativistically corrected Hartree-Fock (HFR) atomic structure code of Cowan.[21] The subshells and their ionization potentials included in the calculation of the direct ionization cross sections are listed in Table I. Direct ionization of the $3s$ electrons from the Kr^{8+} $3d^9 4s$ excited configuration was not included in the calculation because the resulting Kr^{9+} $3s3p^6 3d^9 4s$ configuration is autoionizing, predominantly leading to net double ionization of Kr^{8+}. Likewise, the direct ejection of a $4s$ electron from the Xe^{8+} $4d^9 5s$ excited configuration leads to the autoionizing Xe^{9+} $4s4p^6 4d^9 5s$ configuration, resulting in double ionization. Direct ionization of a $2p$ electron from Kr^{8+} or

TABLE I. Ionization potentials for Kr^{8+} and Xe^{8+}.

Ion	Configuration	Subshell	Configuration-average ionization potential (eV)
Kr^{8+}	$3d^{10}$	$3d$	232.96
		$3p$	359.77
		$3s$	435.95
	$3d^9 4s$	$4s$	147.33
		$3d$	248.40
		$3p$	373.69
Xe^{8+}	$4d^{10}$	$4d$	180.08
		$4p$	274.51
		$4s$	336.45
	$4d^9 5s$	$5s$	122.30
		$4d$	187.36
		$4p$	281.59

a $3d$ electron from Xe^{8+}, in either the ground or excited configurations of the ions, is expected to contribute to double ionization.

The excitation cross sections for transitions to autoionizing levels were also calculated in the configuration-average distorted-wave approximation.[22] For the general transition

$$(n_1 l_1)^{q_1}(n_2 l_2)^{q_2} k_i l_i \rightarrow (n_1 l_1)^{q_1-1}(n_2 l_2)^{q_2+1} k_f l_f \ , \tag{1}$$

where n_j is the principal quantum number, l_j is the angular-momentum quantum number, k_j is the linear momentum of the free electron, and q_j is the occupation number, the configuration-average excitation cross section may be written

$$\sigma_{\text{exc}} = 8\pi q_1 (4l_2 + 2 - q_2)/k_i{}^3 k_f \sum_{l_i l_f} (2l_i+1)(2l_f+1) M(2f;1i) \ , \tag{2}$$

where $M(2f;1i)$, a function of angular coefficients and the Slater radial integrals for Coulomb interaction between electrons, has been expressed in detail previously.[22] The atomic orbitals and bound-state energies required were calculated using the HFR wave-function code of Cowan.[21] A local semiclassical approximation for the exchange interaction[23] was used to calculate the distorted waves (continuum orbitals).

The transitions to autoionizing configurations included in the calculation of the total ionization cross sections are given in Table II, with configuration-average excitation energies and the calculated excitation cross sections at

TABLE II. Excitation cross sections for Kr^{8+} and Xe^{8+} ions in the ground and first-excited configurations. These configuration-average distorted-wave calculations were used in the theory curves of Figs. 2 and 3. The numbers in parentheses indicate, for those transitions which straddle the ionization threshold, the ratio of autoionizing-to-total levels. The excitation cross sections for those transitions were apportioned as explained in the text.

		Avg. excitation energy (eV)		Cross section at threshold (10^{-18} cm^2)	
Ion	Transition	Ground	Excited	Ground	Excited
Kr^{8+}	$3d \rightarrow 4d$		147.8 (85/134)		4.091
	$3d \rightarrow 4f$		175.4		2.139
	$3d \rightarrow 5s$		168.7		0.096
	$3d \rightarrow 5p$		177.1		0.247
	$3d \rightarrow 5d$		190.0		0.930
	$3d \rightarrow 5f$		201.9		0.966
	$3p \rightarrow 4s$		222.8		0.039
	$3p \rightarrow 4p$	232.3 (5/10)	241.0	0.901	0.879
	$3p \rightarrow 4d$	262.2	273.0	0.168	0.160
	$3p \rightarrow 4f$	288.4	300.6	0.155	0.165
	$3p \rightarrow 5s$	281.9	294.0	0.015	0.013
	$3p \rightarrow 5p$	290.0	302.4	0.186	0.170
	$3p \rightarrow 5d$	302.6	315.3	0.059	0.054
	$3p \rightarrow 5f$	314.1	327.2	0.085	0.086
Xe^{8+}	$4d \rightarrow 5f$		130.6		3.688
	$4d \rightarrow 5g$		142.2		0.575
	$4d \rightarrow 6p$		126.2		0.720
	$4d \rightarrow 6d$		137.4		1.985
	$4d \rightarrow 6f$		149.8		1.095
	$4d \rightarrow 6g$		156.1		0.397
	$4p \rightarrow 4f$	180.4 (4/12)	182.4	2.826	2.853
	$4p \rightarrow 5p$		172.6		2.061
	$4p \rightarrow 5d$	193.5	198.6	0.501	0.473
	$4p \rightarrow 5f$	218.9	224.6	0.378	0.327
	$4p \rightarrow 6p$	214.3	220.4	0.408	0.373
	$4p \rightarrow 6d$	225.3	231.6	0.152	0.138
	$4p \rightarrow 6f$	237.5	243.9	0.145	0.126
	$4s \rightarrow 4f$	241.9	245.0	0.383	0.386
	$4s \rightarrow 5s$	214.1		0.388	

threshold. However, for a particular autoionizing configuration, not all levels may lie above the ionization limit. For example, the Kr^{8+} $3d^8 4s 4d$ configuration has 134 levels spread over 21.87 eV, but only 85 of those levels autoionize. To account for this structure within the configurations which straddle the ionization limit, the configuration-average excitation cross section was statistically partitioned over all levels of the final excited configuration. Then the EA cross section for this configuration was summed to include contributions only from levels that autoionize. This procedure could, of course, lead to error for cases where the magnitudes of the cross sections to individual levels are far from statistical.

IV. RESULTS AND DISCUSSION

A. Kr^{8+}

The experimental cross sections for single ionization of Kr^{8+} are given in Table III with one-standard-deviation relative uncertainties. The data are plotted in Fig. 2, along with the results of configuration-average distorted-wave (CADW) calculations of total ionization (direct ionization plus excitation autoionization) for ions in the ground (lower solid curve) and first-excited configurations (upper solid curve). Direct ionization cross sections calculated in the distorted-wave approximation are also shown for the ground-state ion (short-dashed curve) and for the first-excited configuration (long-dashed curve). The Lotz cross section differs from the DW direct ionization cross section for ground-state ions by only a few percent. At energies above 250 eV, the DW direct ionization cross section for ions in the first-excited configuration ($3d^9 4s$) is within 10% of that for the ground-state ions.

The onset of ionization is observed between 144 and 149 eV, as is seen in Fig. 2. Since the ionization potential of ground-state Kr^{8+} is 233 eV, this is clear evidence of metastable ions being present in the beam. As is apparent from the CADW results shown in Fig. 2, the indirect ionization mechanisms are quite different for ions in the ground and first-excited configurations. Near the peak cross section, for example, excitation-autoionization accounts for only 10–15 % of the total ionization from the ground state. From the excited configuration, however, the EA contribution is about 40–45 % of the peak total cross section. The primary reason for this difference is that the monopole $3d \rightarrow 4d$ and dipole $3d \rightarrow 4f$ transitions lead to autoionization from the excited $3d^9 4s$ configuration, but not from the ground $3d^{10}$ configuration. The importance of these two transitions is manifested in their relatively large excitation cross sections (Table II). From the CADW calculations, we estimate that approximately 15% of Kr^{8+} ions in the beam at the collision volume were in metastable levels. A composite cross section based on this metastable fraction is in excellent agreement with the experimental curve at energies below 600 eV, and is in reasonably good agreement at higher energies.

Maxwellian rate coefficients were numerically calculated[24] from the experimental cross sections with a $\ln(E)/E$ dependence used to extrapolate the measured cross sections up to 10^5 eV. The resulting rate coefficients were found to agree with those of Jones and Källne[14] to within 20% over the 100–250-eV range they reported, with the present results being consistently lower. Although these results agree to within the combined reported uncertainties, it should be noted that both the present work and

TABLE III. Experimental electron-impact ionization cross sections for Kr^{8+} and Xe^{8+}. Uncertainties are one-standard-deviation relative only.

Kr^{8+}		Xe^{8+}	
Energy (eV)	Cross section (10^{-18} cm^2)	Energy (eV)	Cross section (10^{-18} cm^2)
124.7	0.03±0.09	87.6	0.46±0.54
134.5	0.06±0.09	97.3	−0.02±0.47
144.4	−0.02±0.08	111.8	0.38±0.73
149.3	0.09±0.05	121.1	1.06±0.58
154.1	0.12±0.05	129.4	2.36±0.58
159.2	0.35±0.07	138.2	2.94±0.69
163.8	0.58±0.05	145.8	2.79±0.50
173.6	0.64±0.06	153.4	2.46±0.48
183.4	0.79±0.06	162.1	2.50±0.63
193.8	0.86±0.06	170.0	3.18±0.36
203.7	0.91±0.06	180.0	3.13±0.23
213.5	1.07±0.06	181.7	2.94±0.36
218.1	1.03±0.06	185.0	5.00±0.44
223.2	1.04±0.05	189.7	5.20±0.34
232.9	1.08±0.05	195.0	5.58±0.46
237.7	1.22±0.05	199.2	5.93±0.32
242.8	1.53±0.04	204.0	6.96±0.35
247.4	1.75±0.06	209.0	7.44±0.35
252.5	1.79±0.06	214.7	7.44±0.29
262.4	2.14±0.06	219.7	7.95±0.20
272.3	2.48±0.06	224.1	7.79±0.27
282.2	2.64±0.06	234.0	8.91±0.30
291.9	2.98±0.06	243.1	9.47±0.18
311.3	3.47±0.06	268.0	9.59±0.22
331.1	3.70±0.05	291.9	9.65±0.23
350.8	3.87±0.04	316.0	10.09±0.19
370.4	4.06±0.05	342.8	10.10±0.16
390.6	4.40±0.06	389.9	10.27±0.12
414.8	4.56±0.05	440.0	10.38±0.12
439.7	4.80±0.06	487.5	10.28±0.13
464.1	4.98±0.05	537.0	10.35±0.12
489.0	5.16±0.05	585.7	9.91±0.11
513.7	5.29±0.05	634.0	9.42±0.13
538.3	5.37±0.05	635.0	9.60±0.08
563.0	5.43±0.04	684.0	9.66±0.07
586.7	5.45±0.05	782.0	9.53±0.11
636.2	5.59±0.04	879.0	8.87±0.13
685.6	5.65±0.03	978.0	8.41±0.12
734.7	5.73±0.03	982.0	8.28±0.15
783.7	5.71±0.04	1081	7.25±0.12
832.9	5.71±0.03	1180	6.63±0.09
882.6	5.66±0.03	1278	6.23±0.09
982.4	5.63±0.03	1377	5.89±0.12
1081	5.46±0.05	1476	5.77±0.11
1179	5.27±0.03		
1277	5.03±0.03		
1375	4.88±0.03		

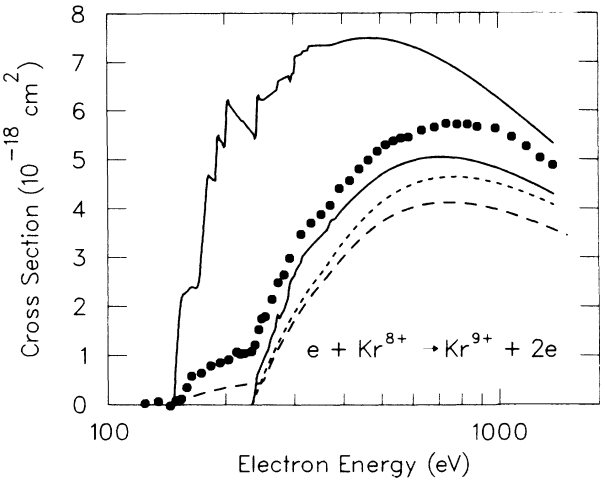

FIG. 2. Single ionization of Kr^{8+} by electron impact. The points are the present data; the dashed curves are CADW calculations of direct ionization from the ground (short-dash) and first-excited (long-dash) configurations; solid curves are CADW calculations for total ionization of ions in ground ($3d^{10}$, lower curve) and first-excited ($3d^9 4s$, upper curve) configurations. Relative uncertainties for the experimental data at the one-standard-deviation level are smaller than the symbol size.

the plasma rate measurements of Jones and Källne are sensitive to the possibly different fractions of metastable ions present in the two experiments.

B. Xe^{8+}

The experimental electron-impact single ionization cross sections for Xe^{8+} are given in Table III with one-standard-deviation relative uncertainties. The data are also plotted in Fig. 3 with configuration-average distorted-wave results for direct ionization of ground-state Xe^{8+} (short-dashed curve) and first-excited configuration (long-dashed curve) ions. Also plotted in Fig. 3 are calculations of total ionization for ions in the ground (lower solid curve) and first-excited (upper solid curve) configurations. The CADW results for direct ionization from the excited configuration ($4d^9 5s$) differ from that for the ground configuration ($4d^{10}$) by less than 10% above 200 eV, but (as was observed for Kr^{8+}) a large difference is observed in that total ionization curves for these configurations.

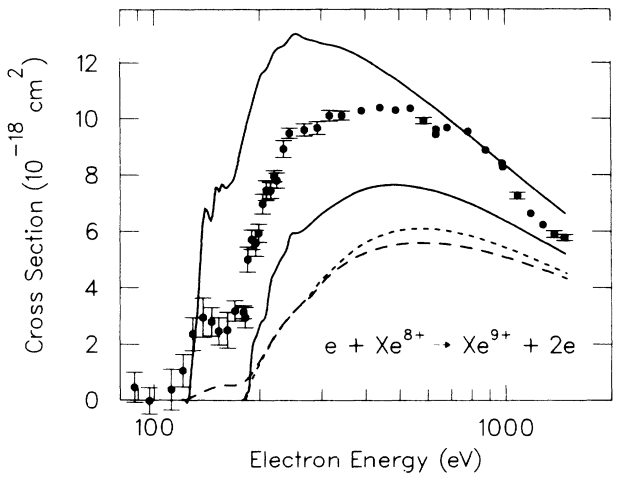

FIG. 3. Single ionization of Xe^{8+} by electron impact. The points are the present data, shown with typical relative uncertainties at the one-standard-deviation level; the dashed curves are DW calculations for direct ionization from the ground (short-dash from Ref. 13 and present results) and first-excited (long-dash) configurations; the solid curves are CADW calculations for total ionization of $4d^{10}$ ground-state (lower curve) and $4d^9 5s$ excited-configuration (upper curve) ions.

The observed threshold for ionization is between 112 and 121 eV, in contrast to the calculated threshold of 182.2 eV for ground-state Xe^{8+}. The configuration-average ionization potential for the first-excited configuration ($4d^9 5s$) of Xe^{8+} was calculated to be 122.3 eV. As was the case for Kr^{8+}, the experimental data reflects the presence of metastable ions in the beam. As has been noted, the total ionization cross section for ions in the first-excited configuration is significantly greater than that of ground-state ions. The difference is primarily due to $4d \rightarrow 5f$ and $4p \rightarrow 5p$ transitions which end in autoionizing levels from the first-excited configuration, but in bound states from the ground state. In addition, all 226 levels of the configuration resulting from $4p \rightarrow 4f$ transitions from the $4d^9 5s$ excited configuration are autoionizing, while only 4 of 12 levels of the final configuration following a $4p \rightarrow 4f$ transition from the ground state are autoionizing. Using the CADW calculations as a guide, we estimate the fraction of metastable ions in the beam to have been about 40%.

V. CONCLUSIONS

The present study has investigated the total cross sections for single ionization of Kr^{8+} and Xe^{8+}. The experiments support theoretical evidence that the contribution to the total ionization cross section due to excitation autoionization is significantly larger from the first-excited configuration than from the ground state. A significant fraction of the target ions were found to be in metastable states, with estimated metastable fractions of 15% and 40% for the Kr^{8+} and Xe^{8+} beams, respectively. The calculation of these fractions, however, is very sensitive to the theoretical cross sections used for comparison, and the resulting metastable fractions should be considered only as rough estimates.

The presence of metastable ions in the collision region has been shown to dramatically affect the measured total ionization cross sections. Thus, the possibility of metastable content must be carefully addressed in treating the ionization of ions for which the excitation-autoionization contributions to total ionization differ significantly between the ground and excited configurations. This has important consequences for the modeling of fusion and x-ray laser plasmas where similar fractions of metastable ions may exist.

ACKNOWLEDGMENTS

The authors acknowledge valuable interactions with R. A. Phaneuf and assistance from H. T. Hunter and J. W.

Hale during the project. This work was supported by the Office of Fusion Energy, U. S. Department of Energy, under Contract No. DE-AC05-840R21400 with Martin Marrietta Energy Systems, Inc. One of us (M.E.B.) acknowledges support from the Magnetic Fusion Science program administered by Oak Ridge Associated Universities for the Office of Fusion Energy of the U.S. Department of Energy. One of us (D.W.M) acknowledges support through the Southern Regional Education Board, the LSU Council on Research, and the Faculty Research Travel Contract Program administered by Oak Ridge Associated Universities for the U. S. Department of Energy under Contract No. DE-AC05-760R00033.

---

*Present address: Princeton Plasma Physics Laboratory, Princeton, NJ 08544.

†Present address: Department of Physics, North Texas State University, Denton, TX 76203.

‡Present address: Department of Physics and Astronomy, Vanderbilt University, Nashville, TN 37235.

§Permanent address: Department of Physics, Auburn University, Auburn, AL 36849.

**Permanent address: Department of Physics, Rollins College, Winter Park, FL 32789.

[1]W. Lotz, Z. Phys. **216**, 241 (1968).

[2]B. Peart and K. T. Dolder, J. Phys. B **1**, 872 (1968).

[3]D. C. Gregory, P. F. Dittner, and D. H. Crandall, Phys. Rev. A **27**, 724 (1983).

[4]A. Matsumoto, S. Ohtani, A. Danjo, H. Hanashiro, T. Hino, Y. Kondo, H. Suzuki, H. Tawara, K. Wakiya, and M. Yoshino, *Abstracts of Contributed Papers, Thirteenth International Conference on the Physics of Electronic and Atomic Collisions, Berlin, 1983,* edited by J. Eichler, W. Fritsch, I. V. Hertel, N. Stolterfoht, and U. Willie (North-Holland, Amsterdam, 1984), p. 198.

[5]A. Danjo, A. Matsumoto, S. Ohtani, H. Suzuki, H. Tawara, K. Wakiya, and M. Yoshino, J. Phys. Soc. Jpn. **53**, 4091 (1984).

[6]D. C. Gregory, Nucl. Instrum. Methods Phys. Res. B **10/11**, 87 (1985).

[7]K. Tinshert, A. Müller, G. Hofmann, C. Achenbach, R. Becker, and E. Salzborn, J. Phys. B **20**, 1121 (1987).

[8]D. C. Gregory and D. H. Crandall, Phys. Rev. A **27**, 2338 (1983).

[9]C. Achenbach, A. Müller, E. Salzborn, and R. Becker, J. Phys. B **17**, 1405 (1984).

[10]D. C. Griffin, C. Bottcher, M. S. Pindzola, S. M. Younger, D. C. Gregory, and D. H. Crandall, Phys. Rev. A **29**, 1729 (1984).

[11]S. Maxon, P. Hagelstein, K. Reed, and J. Scofield, J. Appl. Phys. **57**, 971 (1985); S. Maxon, P. Hagelstein, J. Scofield, and Y. Lee, *ibid.* **59**, 293 (1986).

[12]B. J. MacGowan, S. Maxon, P. L. Hagelstein, C. L. Keane, R. A. London, D. L. Matthews, M. D. Rosen, J. H. Scofield, and D. A. Whelan, Phys. Rev. Lett. **59**, 2157 (1987).

[13]S. M. Younger, Phys. Rev. A **34**, 1952 (1986).

[14]L. A. Jones and E. Källne, J. Quant. Spectrosc. Radiat. Transfer **30**, 317 (1983).

[15]H. J. Kunze, Phys. Rev. A **3**, 937 (1977).

[16]F. W. Meyer, Nucl. Instrum. Methods Phys. Res. B **9**, 532 (1985).

[17]P. O. Taylor, K. T. Dolder, W. E. Kauppila, and G. H. Dunn, Rev. Sci. Instrum. **45**, 538 (1974).

[18]D. C. Gregory, F. W. Meyer, A. Müller, and P. Defrance, Phys. Rev. A **34**, 3657 (1986).

[19]S. M. Younger, Phys. Rev. A **22**, 111 (1980).

[20]M. S. Pindzola, D. C. Griffin, and C. Bottcher, J. Phys. B **16**, L355 (1983).

[21]R. D. Cowan, *The Theory of Atomic Structure and Spectra* (California Press, Berkeley, 1981); R. D. Cowan and D. C. Griffin, J. Opt. Soc. Am. **66**, 1010 (1976).

[22]M. S. Pindzola, D. C. Griffin, and C. Bottcher, Phys. Rev. A **33**, 3787 (1986).

[23]M. E. Riley and D. G. Truhlar, J. Chem. Phys. **63**, 2182 (1975).

[24]The program is briefly described in Ref. 18; for more details, see M. S. Pindzola, D. C. Griffin, C. Bottcher, S. M. Younger, and H. T. Hunter, Nucl. Fusion, Special Suppl., p. 21 (1987).